Proceedings of the Thirty-second (2022) International Ocean and Polar Engineering Conference **www.isope.org**
Shanghai, China, June 5–10, 2022

ISBN 978-1-880653-81-4; ISSN 1098-6189

Numerical simulation of irregular waves by HOS method

Congyi Huang[1], *Ping Xu*[2], *Decheng Wan*[1*], *Sergei Strijhak*[3]

[1] Computational Marine Hydrodynamic Lab (CMHL), School of Naval Architecture, Ocean and Civil Engineering, Shanghai Jiao Tong University, Shanghai, China
[2] Marine Design and Research Institute of China, Shanghai, China
[3] Ivannikov Institute for System Programming of the Russian Academy of Sciences, Moscow, Russia
[*]Corresponding author

ABSTRACT

Ships and offshore structures often encounter irregular waves in the ocean. Therefore, the simulation of irregular waves is very necessary and meaningful. The potential flow method is often used to simulate the irregular waves because the evolution needs a long time and a large amount of calculation. High order spectral (HOS) method is a kind of potential flow method, which has the advantages of high efficiency. In this paper, the HOS method is used to simulate the formation and evolution of irregular waves. Firstly, the governing equations, boundary conditions and the solving procedure of the HOS-ocean model based on the HOS method are introduced. Then the accuracy and stability of the HOS-ocean model are verified by a standard example. After that, the formation and evolution of two-dimensional and three-dimensional irregular waves are simulated based on JONSWAP spectrum and ITTC spectrum respectively. The frequency domain curves, time domain curves, maximum wave height, maximum wave steepness, average wave steepness and other parameters of the waves generated by the two wave spectrums are compared, and the differences between the two wave spectrums in generating irregular waves are analyzed.

KEY WORDS: Higher order spectral method; Potential flow method; Irregular waves; JONSWAP spectrum; ITTC spectrum.

INTRODUCTION

High-order Spectrum (HOS) method is a kind of pseudo-spectral method (PSM), which is based on the potential flow theory. This method can efficiently simulate the generation and evolution of nonlinear waves by pseudo-spectral expansion and fast Fourier transform (FFT). Firstly, the velocity potential perturbation is expanded into a series of characteristic functions, and then the derivative term is solved by FFT. This method has high computational accuracy and efficiency, so it is widely used in the simulation of nonlinear waves.

HOS method was first proposed by West (1987) and Dommermuth and Yue (1987) respectively in the same year, and was initially used to simulate nonlinear gravity waves. At that time, HOS method could only be used to simulate deep water waves under two-dimensional periodic boundary conditions. Subsequently, Liu and Dommermuth (1992) further extended the HOS method on the basis of the previous work. The diffraction interaction between three-dimensional nonlinear wave and submerged objects was simulated, and the calculated results agreed well with the experimental data. In order to avoid the calculation errors caused by the direct nonlinear evolution of the initial wave surface, Dommermuth (1999) adopted a relaxation scheme to make the linear initial wave smoothly transferred to nonlinear in a specific period of time. Tanaka (2000) introduced the wave spectrum function and the initialization of HOS calculation directly based on the wave spectrum was realized. Bonnefoy (2004) considered the aliasing error caused by the time-domain and frequency-domain transformation. He introduced an aliasing elimination method that allowed long-time evolution based on wave spectrum. Ducrozet et al. (2007) simulated the wave field based on JONSWAP spectrum in a large area (thousands of square kilometers) for a long time (nearly three hours). The generation probability of extreme waves and the change of characteristic morphology were explored under the influence of different wave directional parameters. Ducrozet (2012) proposed a three-dimensional nonlinear numerical pool based on HOS method. The model can be used for wave generation with push plate and swing plate based on nonlinear wave generation boundary. The wave generation results of the numerical pool were in good agreement with the laboratory pool, which verified the accuracy and validity. Ducroze et al. (2016) developed HOS-ocean, an open source solver for the evolution of nonlinear waves in the open sea. Song et al. (2018) introduced ITTC two-parameter spectrum into the HOS-ocean solver based on previous work. The two-parameter spectrum of ITTC was analyzed, the focused wave was simulated, and the multi-directional irregular wave was studied. Zhuang et al. (2018) coupled the HOS method with the CFD method and conducted 2D and 3D simulation verification of regular and irregular waves.

In this paper, the basic theoretical equations and solving process of HOS method are introduced. Then the boundary conditions and initialization process of the HOS-ocean solver used in this paper are introduced. After that, the wave evolution in open water is analyzed based on JONSWAP

spectrum and ITTC two-parameter spectrum respectively. Firstly, the accuracy of JONSWAP spectrum and ITTC spectrum are verified respectively. Then, two-dimensional and three-dimensional irregular waves are generated based on the two wave spectrums above respectively. By comparing the time domain curves, frequency domain curves, maximum wave height, maximum wave steepness, average wave steepness and other parameters, the differences between the two wave spectrums are analyzed. Finally, the applicable conditions of the two wave spectrums are simply inferred.

NUMERICAL METHOD

Mathematical equations for HOS method

Based on potential flow theory, the HOS method studies the non-rotational and isotropic flow field composed of inviscid and incompressible fluid, and the velocity potential satisfies Laplace equation, as shown in Eq.1.

$$\nabla^2\Phi(x,z,t)=0 \tag{1}$$

The dynamic conditions and kinematic conditions at the free surface $z=\eta(x,t)$ are shown in Eq.2 and Eq.3,

$$\Phi_t+gz+\frac{1}{2}(\nabla\Phi)^2=0 \tag{2}$$

$$\eta_t+\nabla_x\eta\cdot\nabla_x\Phi=\Phi_z \tag{3}$$

Where $\nabla_x\equiv\left(\frac{\partial}{\partial x},\frac{\partial}{\partial y}\right)$ represents the horizontal gradient.

Referring to Zakharov (2009), the surface velocity potential can be written as:

$$\Phi^s(x,y,t)=\Phi[x,\eta(x,t),t] \tag{4}$$

Thus, the kinematic and dynamic boundary conditions on the free surface can be expressed as:

$$\Phi_t^s+g\eta+\frac{1}{2}(\nabla_x\Phi^s)^2-\frac{1}{2}(1+(\nabla\eta)^2)\Phi_z^2(x,\eta,t)=0 \tag{5}$$

$$\eta_t+\nabla_x\Phi^s\cdot\nabla_x\eta-(1+(\nabla_x\eta)^2)\Phi_z(x,\eta,t)=0 \tag{6}$$

With the use of perturbation expansion, the velocity potential can be written as:

$$\Phi(x,z,t)=\sum_{m=1}^{M}\Phi^{(m)}(x,z,t) \tag{7}$$

Perform each $\Phi^{(m)}$ evaluated on $z=\eta$ by Taylor expansion around z=0 and retain to the same order M, Eq.8 can be obtained:

$$\Phi^s(x,t)=\Phi(x,\eta,t)=\sum_{m=1}^{M}\sum_{k=0}^{M-m}\frac{\eta^k}{k!}\frac{\partial^k}{\partial z^k}\Phi^{(m)}(x,0,t) \tag{8}$$

For a given moment t, both Φ^s and η are considered to be known. The wave surface information for the next time step can be obtained by using Eq.5 and Eq.6. Expansion Eq.8, combining the terms of the same order, a series of boundary conditions about $\Phi^{(m)}$ at z = 0 can be obtained.

$$\Phi^{(1)}(x,y,0,t)=\Phi^s(x,y,t) \tag{9}$$

$$\Phi^{(m)}(x,y,0,t)=-\sum_{k=1}^{m-1}\frac{\eta^k}{k!}\frac{\partial^k}{\partial z^k}\Phi^{(m-k)}(x,y,0,t)\ \ m=2,3,\cdots,M \tag{10}$$

Eq.9 and Eq.10 are a series of Dirichlet boundary conditions satisfied at z=0. It is assumed that the eigen function $\psi_n(x,y,z),z\le 0$ is known and satisfies Laplace equation and boundary conditions, but does not satisfy Dirichlet's free surface condition. Thus we can expand the velocity potential $\Phi^{(m)}$ by the eigen function and truncate it at the appropriate number of modes, which can be written as:

$$\Phi^{(m)}(x,y,z,t)=\sum_{m=0}^{N}\Phi_n^{(m)}(t)\psi_n(x,y,z),z\le 0 \tag{11}$$

Using Eq.11, we can get:

$$\Phi_z(x,y,\eta,t)=\sum_{m=1}^{M}\sum_{k=0}^{M-m}\frac{\eta^k}{k!}\sum_{n=1}^{N}\Phi_n^{(m)}(t)\frac{\partial^{k+1}}{\partial z^{k+1}}\psi(x,y,0) \tag{12}$$

Substituting Eq.12 into Eq.5 and Eq.6, we can get:

$$\eta_t+\nabla\Phi^s\cdot\nabla\eta-(1+\nabla\eta\cdot\nabla\eta)*\left[\sum_{m=1}^{M}\sum_{k=0}^{M-m}\frac{\eta^k}{k!}\sum_{n=1}^{N}\Phi_n^{(m)}(t)\frac{\partial^k}{\partial^{k+1}}\psi_n(x,y,0)\right]=0 \tag{13}$$

$$\Phi_t^s+\frac{1}{2}\nabla\Phi^s\cdot\nabla\Phi^s-\frac{1}{2}(1+\nabla\eta\cdot\nabla\eta)*\left[\sum_{m=1}^{M}\sum_{k=0}^{M-m}\frac{\eta^k}{k!}\sum_{n=1}^{N}\Phi_n^{(m)}(t)\frac{\partial^k}{\partial^{k+1}}\psi_n(x,y,0)\right]^2=0 \tag{14}$$

Eq.13 and Eq.14 are the evolution equations of surface velocity potential Φ^s and height η expressed by mode amplitude $\Phi_n^{(m)}$. By solving these two equations, the time derivatives of wave height η and surface velocity potential Φ^s at this time step, η_t and Φ_t^scan be obtained. Then the wave height and surface velocity potential at the next moment can be obtained by time stepping method.

IRREGULAR WAVE SIMULATION BASED ON HOS

In this section, the long-time evolution of nonlinear waves in open water is carried out by the HOS-ocean model. Firstly, the initialization method of HOS-ocean model based on wave spectrum is introduced, and the spectral density function of JONSWAP spectrum and ITTC two-parameter spectrum are introduced respectively. Then the evolution process of two-dimensional and three-dimensional nonlinear irregular waves is simulated based on JONSWAP and ITTC respectively. The time domain curve and frequency domain curve of wave height at the measurement point are compared, and the differences between two-dimensional irregular waves and three-dimensional irregular waves are analyzed. Finally, the differences between JONSWAP spectrum and ITTC spectrum in wave generation are analyzed.

Introduction of wave spectrum

Since the HOS-ocean model does not have a wave-making module, the initialization of wave field can only be completed by presetting the wave height and velocity potential at the initial moment. In this paper, the initial wave field is obtained by wave spectrum. Wave spectrum is defined by multidirectional spectral density function, expressed as:

$$S(\omega,\theta)=F(\omega)G(\theta) \tag{26}$$

In the formula, $F(\omega)$ represents the spectral density distribution function and describes the proportion of wave composition with specific frequency ω, which is used to distinguish different types of wave spectrum. $G(\theta)$ represents the direction distribution function and distinguishes the directionality of irregular waves. In this paper, only the one-direction wave is simulated, so the influence of $G(\theta)$ is not considered. According to Tanaka (2001), the amplitude B_{mn} of each

wave component in discrete Fourier calculation can be obtained, so as to determine the amplitude of wave height and velocity potential of each wave component. Then the information in space domain can be obtained by FFT, and the wave height and velocity potential distribution at the initial time can be obtained by linear superposition.

The spectral density function $F_J(\omega)$ of JONSWAP can be expressed as:

$$F_J(\omega) = C_J \omega^{-5} \exp\left(-\frac{5}{4\omega^4}\right) \gamma^{\exp[-(\omega-1)^2/2\sigma^2]} \tag{27}$$

$$C_J = 3.279E, \gamma = 3.3, \sigma = \begin{cases} 0.07(\omega < 1) \\ 0.09(\omega \geq 1) \end{cases} \tag{28}$$

where γ is the spectral amplification factor, with a general value of 3.3. E represents the energy density of the wave field, which can be estimated by $H_s \approx 4\sqrt{E}$. H_s stands for significant wave height.

The spectral density function $F_I(\omega)$ of the standardized ITTC two-parameter spectrum can be written as

$$F_I(\omega) = \frac{173 \cdot (16E)}{(0.78T_p)^4 \omega^5} \exp\left(-\frac{691}{(0.78T_p)^2 \omega^4}\right) \tag{29}$$

where T_p is the spectral peak period.

Irregular wave simulation based on JONSWAP

In this section, two-dimensional and three-dimensional irregular waves are simulated respectively based on JONSWAP. The significant wave height $H_s = 2.8m$, the spectral peak period $T_p = 10s$, and the spectral peak frequency is $\omega = 2\pi/T_p \approx 0.628s$. The size of the compute domain is $L_x = L_y = 11\lambda_p$, λ_p is the characteristic wavelength. According to Bonnefoy (2001), λ_p is related to the spectral peak period T_p. In this paper, $\lambda_p \approx 141.94m$. The simulation time $T = 100T_p = 1000s$, the order of HOS is M=5. The wave probe is located in the center of the computing domain, $X_p = 5.5\lambda_p$. Firstly, the frequency domain curve of the wave is drawn and compared with the theoretical value, as shown in Fig.1.

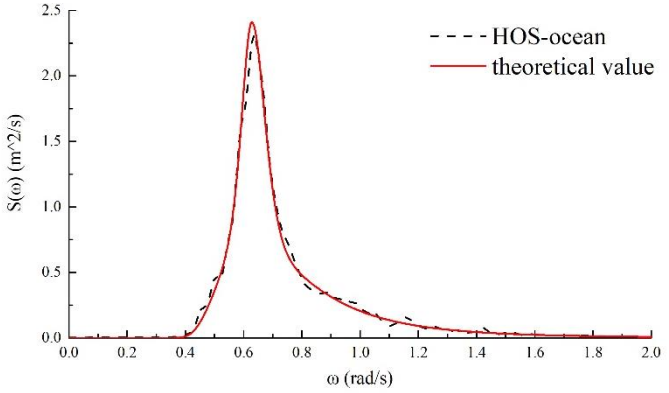

Fig.1 The simulating spectrum compared with the theoretical JONSWAP spectrum

It can be seen from Fig.1 that the two-dimensional irregular wave simulated based on JONSWAP spectrum is in good agreement with the theoretical value. The spectral peak frequency is about 0.628, which is consistent with the theoretical value. The accuracy of HOS-ocean model and JONSWAP spectrum is verified.

The time domain curves for the height of two-dimensional and three-dimensional irregular wave based on JONSWAP are shown in Fig.2 and Fig.3. The horizontal coordinate represents time, and the y-coordinate represents a dimensionless parameter η/H_s.

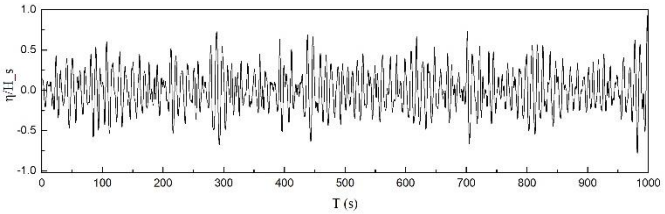

Fig.2 Surface elevation record of 2D wave field based on JONSWAP spectrum

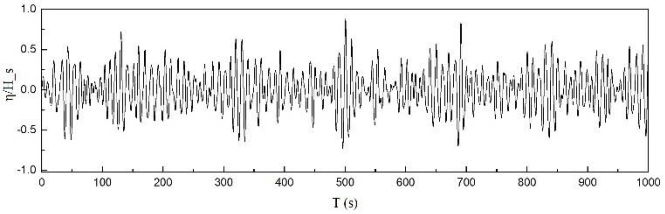

Fig.3 Surface elevation record of 3D wave field based on JONSWAP spectrum

As can be seen from Fig.2 and Fig.3, there is no obvious difference between the two-dimensional and three-dimensional irregular waves generated based on JONSWAP, and both of them can represent the nonlinear characteristics. Fig.4 shows the wave field of three-dimensional irregular waves at different times.

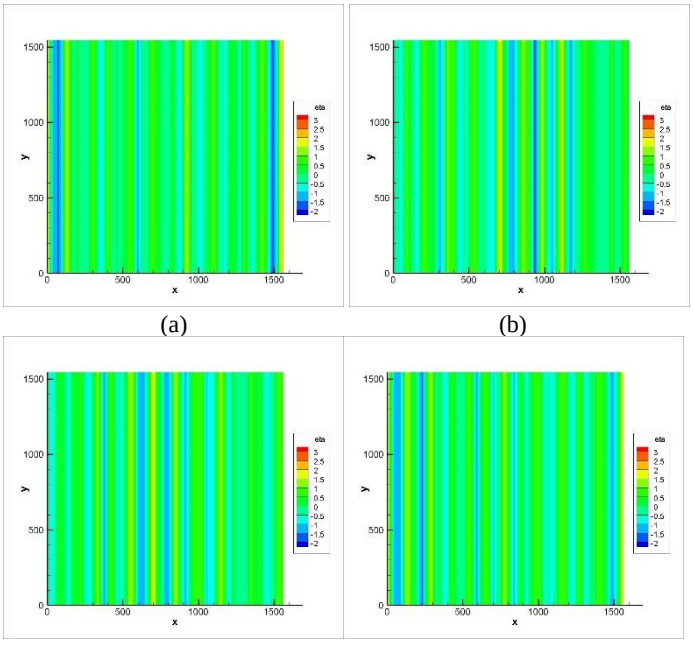

Fig.4 Distribution of wave height by JONSWAP at different times. (a) t=2.5T_p; (b) t=5T_p; (c) t=7.5T_p; (a) t=10T_p.

The maximum wave height of two-dimensional irregular wave based on JONSWAP appears at t = 275.2s, and the maximum wave height is 2.97m. The wave field at this time is shown in Fig.5. The maximum wave height appears at x = 1389.89m, which is approximately 9.79λ_p away

from the inlet. And the maximum wave height of the three-dimensional irregular wave based on JONSWAP is 2.59m at t = 511.2s. The wave field at this time is shown in Fig.6. Since the generated irregular waves are unidirectional waves, the wave has the same distribution in the y direction, and the maximum wave height appears at the position of x = 30.6144m, approximately $0.22\lambda_p$ away from the entrance. Therefore, it can be analyzed that for the irregular wave generated based on JONSWAP, the maximum wave height of three-dimensional wave is slightly lower than that of two-dimensional wave, and appears slightly later.

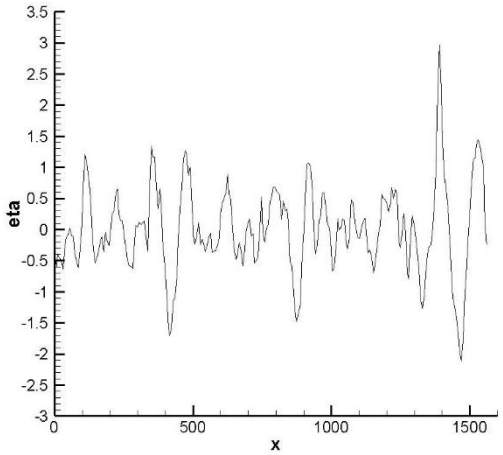

Fig.5 Wave field of two-dimensional irregular wave based on JONSWAP at t = 275.2s with the peak value of 2.97m.

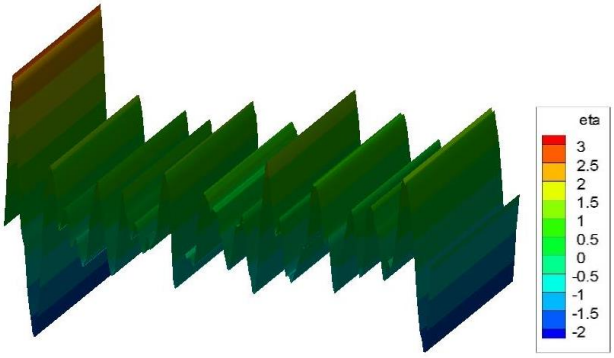

Fig.6 Wave field of three-dimensional irregular wave based on JONSWAP at t = 511.2s with a peak value of 2.59m.

The wave height curves in time-domain of two-dimensional and three-dimensional irregular waves are analyzed respectively, and the frequency-domain curves are obtained. Compare the frequency domain curves of two-dimensional and three-dimensional irregular waves, as shown in Fig.7.

As can be seen from Fig.7, the frequency domain curves of two-dimensional and three-dimensional waves have few differences, and their spectral peak frequencies approximately coincide. Compared with the two-dimensional waves, the frequency domain spectrum of three-dimensional waves is of higher peak value and narrow range of data distribution. In general, the frequency domain curves of two-dimensional irregular waves and three-dimensional irregular waves are roughly consistent. So it can be considered that the dimension has little effect when simulating irregular wave based on JONSWAP spectrum.

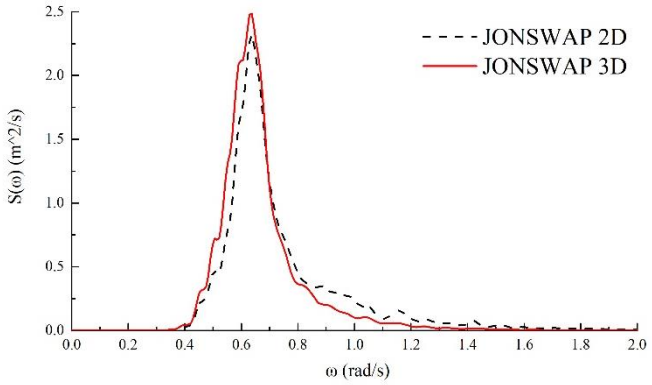

Fig.7 Comparison of 2D and 3D wave frequency domains based on JONSWAP

Irregular wave simulation based on ITTC

Next, the ITTC two-parameter spectrum is used to simulate two-dimensional and three-dimensional irregular waves. The calculation domain scale, wave parameters, calculation time and other parameters in this section are consistent with the simulation based on JONSWAP, and the location of measuring points is also the same. The frequency domain curve of the wave is drawn and compared with the theoretical value, as shown in Fig.8.

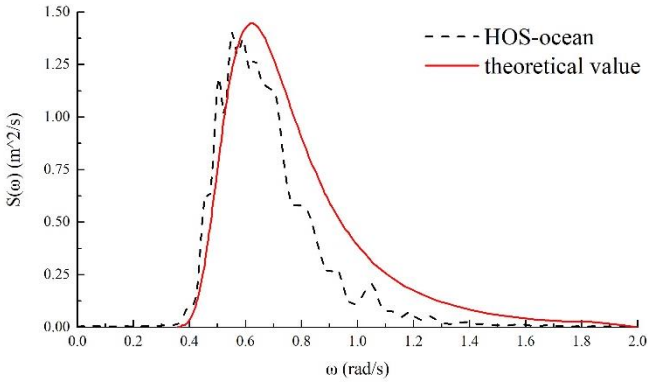

Fig.8 The simulating spectrum compared with the theoretical ITTC spectrum

As can be seen from Fig.8, the shape of the theoretical curve and the curve obtained based on ITTC are roughly the same, and the peak value of the frequency domain curves are very close, but the spectral peak frequency are slightly different. The spectral peak frequency of three-dimensional irregular wave based on ITTC is slightly less than the theoretical value, about 0.6 rad/s, but the theoretical value is about 0.628 rad/s. In general, the simulation based on ITTC is effective and accurate, but it is not as good as that based on JONSWAP spectrum.

The time domain curve of wave height recorded by the wave probe is shown in Fig.9 and Fig.10. It can be seen from the figure that there is no obvious difference between two-dimensional and three-dimensional irregular waves generated based on ITTC spectrum, and both can reflect the nonlinear characteristics of irregular waves. The amplitude of three-dimensional wave is slightly smaller than that of two-dimensional wave. Fig.11 shows the wave field of three-dimensional irregular waves at different times.

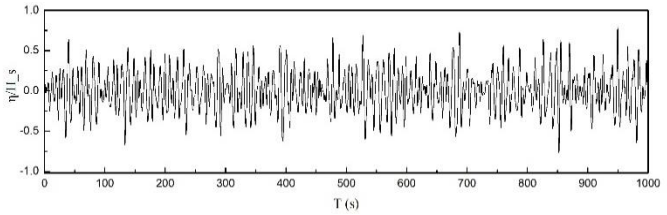

Fig.9 Surface elevation record of 2D wave field based on ITTC spectrum

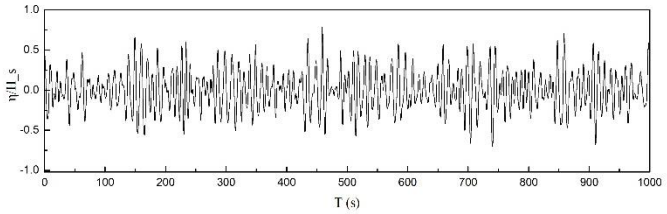

Fig.10 Surface elevation record of 3D wave field based on ITTC spectrum

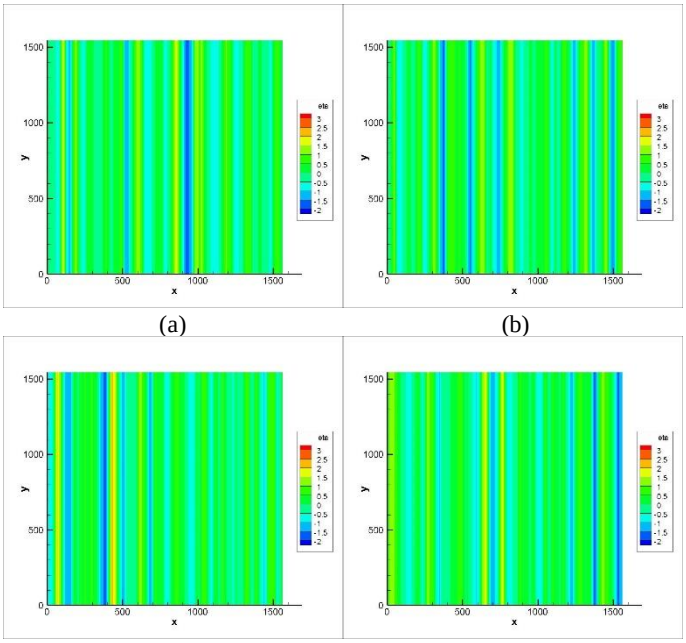

Fig.11 Distribution of wave height at different times. (a) t=2.5T_p; (b) t=5T_p; (c) t=7.5T_p; (a) t=10T_p.

The maximum wave height of the two-dimensional irregular wave generated based on ITTC appears at t = 511.2s and the maximum wave height is 3.32m. The wave field at this time is shown in Fig. 12. The maximum wave height appears at x = 1144.98m, which is approximately 8.06 λ_p away from the inlet. The maximum wave height of three-dimensional irregular wave appears when t = 24s, and the value is 3.15m. At this time, the wave field is shown in Fig.13 The maximum wave height appears at the position of x = 361.25m, which is approximately 2.545λ_p away from the entrance.

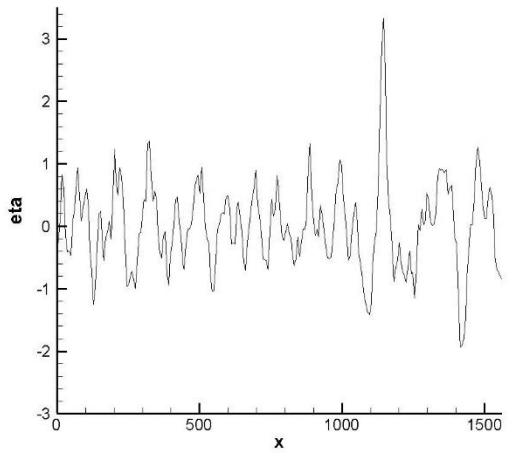

Fig.12 Wave field of two-dimensional irregular wave based on ITTC at t = 511.2s with a peak value of 3.32m

Like the irregular waves generated based on JONSWAP, for ITTC, the maximum wave height of three-dimensional waves is slightly lower than that of two-dimensional waves. However, the maximum wave appears very early at t=24s. It can be guessed that the time when the max wave height appears should be random, independent of the dimension. We can also find that the maximum wave of two-dimensional irregular waves often appears on the side away from the entrance and close to the exit, while the maximum wave of three-dimensional irregular waves often appears on the side close to the entrance and far from the exit.

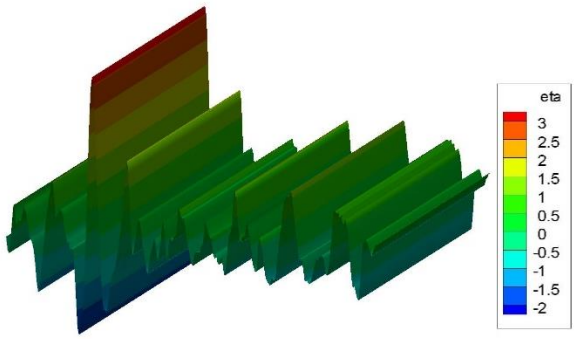

Fig.13 Wave field of three-dimensional irregular wave based on ITTC at t = 24s with a peak value of 3.15m

In order to study the difference of wave generation based on HOS-ocean in generating waves with different dimensions, the frequency domain curves of two-dimensional and three-dimensional irregular waves are obtained by FFT. The comparison the two frequency domain curves is shown in Fig.14.

As can be seen from Fig.14, the frequency domain curves of two-dimensional and three-dimensional irregular waves obtained by ITTC spectrum are partially different. Compared with two-dimensional irregular wave, three-dimensional irregular wave has larger spectral peak and lower spectral peak frequency. Moreover, the spectrum of three-dimensional irregular waves is more concentrated and closer to the theoretical value. Therefore, it can be considered that when simulating irregular waves based on ITTC spectrum, the simulation of three-dimensional irregular waves is better than that of two-dimensional irregular waves.

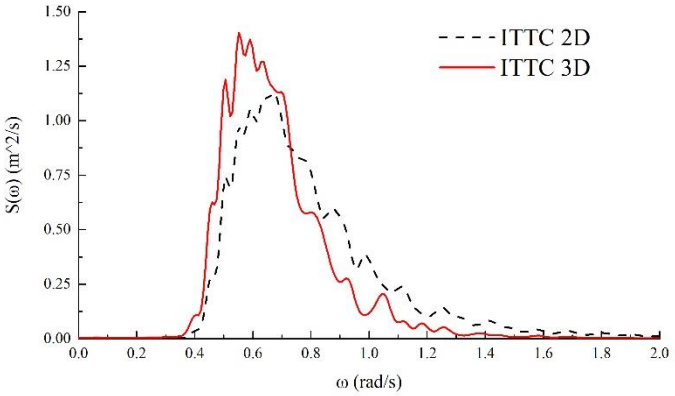

Fig.14 Comparison of 2D and 3D wave frequency domains based on ITTC

Comparison between the simulation based on JONSWAP and ITTC

Firstly, the differences of the wave surface shape based on JONSWAP and ITTC are analyzed. The maximum wave height H_{max}, the time t and location x_{max} of the maximum wave, and the average wave steepness $\bar{\delta}$ and maximum wave steepness δ_{max} of the wave field at this time are summarized in Table 1. It can be seen from Table 1 that for both two-dimensional and three-dimensional waves, the maximum wave height based on ITTC spectrum is larger than that of JONSWAP spectrum. The average wave steepness $\bar{\delta}$ of the waves based on ITTC is also larger than that of JONSWAP whether for the two-dimensional waves or three-dimensional waves. However, for the maximum wave steepness δ_{max} , the results of ITTC are larger in three-dimensional waves and JONSWAP are larger in two-dimensional waves. It can be considered that the amplitude of waves generated based on ITTC spectrum is larger than that of JONSWAP. We can also see from Table 1 that the maximum wave height H_{max}, maximum wave steepness δ_{max} and average wave steepness $\bar{\delta}$ of two-dimensional waves are larger than those of three-dimensional waves.

Table 1. Statistics of maximum wave height, wave steepness and other relevant parameters

	H_{max}/m	x_{max}/λ_p	t/s	$\bar{\delta}$	δ_{max}
JONSWAP 2D	2.97	9.79	275.2	0.038	0.135
ITTC 2D	3.32	8.06	511.2	0.047	0.116
JONSWAP 3D	2.59	0.22	502.8	0.025	0.055
ITTC 3D	3.15	2.545	24	0.028	0.096

Then, the two-dimensional and three-dimensional wave frequency domain curves obtained by JONSWAP spectrum and ITTC spectrum are compared to analyze the differences between the two wave spectrums in generating irregular waves.

Fig.15 shows the comparison of two-dimensional irregular wave frequency domain curves generated by JONSWAP spectrum and ITTC spectrum, and Fig.16 shows the comparison of three-dimensional irregular wave frequency domain curves generated by JONSWAP spectrum and ITTC spectrum. It can be seen from the figure that there are few differences between the spectral peak frequencies of the two wave spectrums, whether for two-dimensional waves or three-dimensional waves. For two-dimensional waves, the frequencies of wave components of irregular wave obtained by two wave spectrums are both about 0.4rad/s to 1.8rad/s, while for three-dimensional waves, the frequency of the wave components is about 0.4rad/s to 1.3rad/s. Therefore, it can be considered that when the HOS-ocean model simulates irregular waves, the frequency distribution of the three-dimensional irregular wave components is narrower, and the frequency distribution of the two-dimensional irregular components waves is wider. For the two wave spectrums used in this paper, when simulating irregular waves, the wave frequency range of the components is basically the same. However, the peaks of the frequency domain curves of the waves generated by the two wave spectrums are quite different. The peak curve value of irregular waves obtained by ITTC spectrum is only about 50% of JONSWAP spectrum, whether for two-dimensional waves or three-dimensional waves. Moreover, the frequency domain curves of irregular wave obtained by ITTC is not as concentrated as that obtained by JONSWAP, which may because that there is a spectral amplification factor in JONSWAP spectrum, which will make the components of irregular wave more concentrated in frequency.

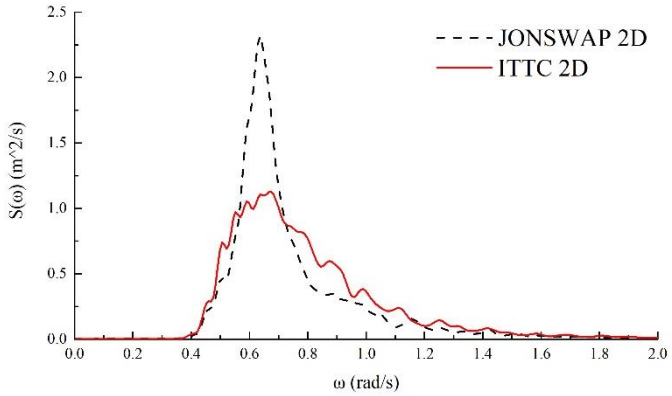

Fig.15 Comparison of 2D wave spectrum based on JONSWAP and ITTC

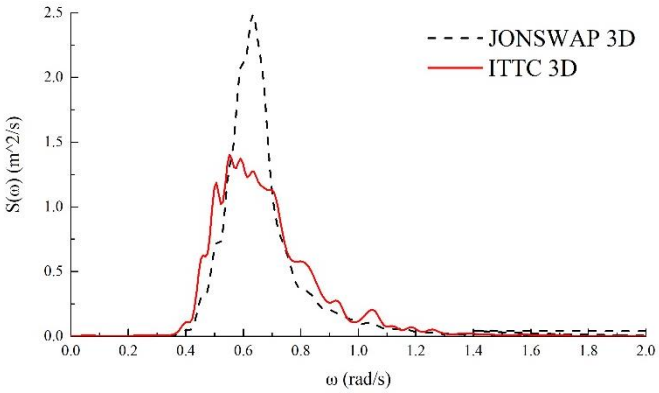

Fig.16 Comparison of 3D wave spectrum based on JONSWAP and ITTC

CONCLUSIONS

In this paper, the HOS-ocean model is used to simulate the long-term evolution of irregular waves in open water based on two kinds of wave spectrums, JONSWAP and ITTC. The differences between the simulations based on these two spectrums are analyzed. When simulating irregular waves, the time-domain curves can obviously show the nonlinear characteristics. Moreover, the frequency domain curves of wave are in good agreement with the theoretical curves of wave spectrum, which verifies the effectiveness and accuracy of the method. By

comparing the wave height and occurrence time of the maximum wave, it can be found that the maximum wave height by JONSWAP is higher and the wave spectrum peak is larger compared with ITTC, which is about twice more than that of ITTC. The average wave steepness $\bar{\delta}$ and maximum wave steepness δ_{max} of the waves generated based on ITTC are also larger than those generated by JONSWAP spectrum. And for the frequency domain curves, the frequency distribution of wave components based on JONSWAP is more concentrated. This may because that there is a spectral amplification factor in JONSWAP spectrum.

Based on the above analysis, we can infer the applicability of JONSWAP spectrum and ITTC two-parameter spectrum. As we all know, JONSWAP spectrum is more suitable for windy sea areas. The characteristic of this wave spectrum is that the peak value is high and the frequency distribution of wave components is narrow. While ITTC two-parameter spectrum is more suitable for fully developed waves with lower peak value and slightly wider frequency distribution. As can be seen from the simulation results in this paper, the average wave steepness, maximum wave steepness and maximum wave height generated by ITTC are all larger than that of JONSWAP. Therefore, if the steeper waves need to appear in the wave field, or if it is necessary to simulate the situation with stronger nonlinearity, the ITTC two parameter spectrum may be a better choice.

ACKNOWLEDGEMENTS

This work was supported by the National Natural Science Foundation of China (51879159, 52131102), and the National Key Research and Development Program of China (2019YFB1704200), to which the authors are most grateful.

REFERENCES

Bonnefoy F, Touz L, Ferrant P (2004). "Generation of fully-nonlinear prescribed wave fields using a high-order spectral model," *Proc 14th Int Offshore and Polar Eng Conf*, ISOPE, 4(1), 234-252.

Bonnefoy F, Ducrozet G, Le Touzé D, et al (2010). "Time domain simulation of nonlinear water waves using spectral methods," *Advances in Numerical Simulation of Nonlinear Water Waves*: 129-164.

Dommermuth D (2000). "The initialization of nonlinear waves using an adjustment scheme," *Wave Motion*, 32(4): 307-317.

Dommermuth D G, Yue D K P (1987). "A High-Order Spectral Method for the Study of Nonlinear Gravity Waves," Journal of Fluid Mechanics, 184: 267-288.

Ducrozet G, Bonnefoy F, LE Touzé D, et al (2007). "3-D HOS simulations of extreme waves in open seas," *Natural Hazards and Earth System Science*, 7(1):109-122.

Ducrozet G, Bonnefoy F, Le Touzé D, et al (2012). "A modified high-order spectral method for wave maker modeling in a numerical wave tank," *European Journal of Mechanics-B/Fluids*, 34: 19-34.

Ducrozet G, Bonnefoy, Félicien, Le Touzé, David, et al (2016). "HOS-ocean: Open-Source Solver for Nonlinear Waves in Open Ocean Base on High-Order Spectral Method," *Computer Physics Communications*: S0010465516300327.

Liu Y, Dommermuth D G, Yue D K P (1992). "A high-order spectral method for nonlinear wave-body interactions," *Journal of fluid Mechanics*, 245: 115-136.

Song J, Zhuang Y, Wan D (2018). "New Wave Spectrums Models Developed Based on HOS Method," *International Ocean and Polar Engineering Conference*, Sapporo, Japan, pp.524-531.

Tanaka M (2001). "Verification of Hasselmann's energy transfer among surface gravity waves by direct numerical simulations of primitive equations," *Journal of Fluid Mechanics*, 444: 199-221.

West B J, Brueckner K A, Janda R S, et al (1987). "A New Numerical Method for Surface Hydrodynamics," *Journal of Geophysical Research: Ocean*, 92.

Zakharov V E, Ostrovsky L A (2009). "Modulation instability: the beginning," *Physica D: Nonlinear Phenomena*, 238(5): 540-548.

Zhuang Y, Wan D, Bouscasse B, Ferrant P (2018). "Regular and Irregular Wave Generation in OpenFOAM using High Order Spectral Method," *The 13th OpenFOAM Workshop*, Shanghai, China, pp.182-192.